



# Atomic Mixing Behavior of Co/Al(001) vs. Al/fcc-Co(001): Molecular Dynamics Simulation

SANG-PIL KIM,<sup>1,2</sup> SEUNG-CHEOL LEE,<sup>2</sup> KWANG-RYEOL LEE<sup>2</sup> & YONG-CHAE CHUNG<sup>1,\*</sup>

<sup>1</sup>*CPRC, Department of Ceramic Engineering, Hanyang University, Seoul 133-791, Korea*

<sup>2</sup>*Future Technology Research Division, Korea Institute of Science and Technology, Seoul 130-650, Korea*

Submitted March 3, 2003; Revised February 4, 2004; Accepted April 30, 2004

**Abstract.** Using molecular dynamics simulations, we investigated the interface structures and the growth behaviors of nano-scale Al/Co/Al multilayers. For Co on Al(001), interface mixing occurred irrespective of the incident energy ( $K_i$ ). Interestingly, increasing the incident energy increased the thickness of the mixing layers and decreased the roughness of the Co surface. In the case of Al on Co(001), in contrast to the case of Co/Al, interface mixing could not be found, especially for low incident energy. From these investigations, an optimized deposition technique is proposed that improves the quality of the interface/surface of the deposited thin film by controlling the incident adatom energies.

**Keywords:** Al/Co/Al, magnetic nano thin films, interface structure, molecular dynamics simulation

## 1. Introduction

Nano-scale multilayers have various interesting structural and electro-magnetic properties and have been employed in many applications. For example, most of the magnetic devices have a sandwich structure that is composed of magnetic/nonmagnetic thin films such as Co/Si/Co, Fe/SiFe/Fe, Au/Co/Au, Cu/Fe/Cu, Rh/Co/Rh, or Ta/Co/Ta [1–6]. For MRAM applications, ordered and uniform thin films less than 1–2 nm thick are especially required for the coherency of the device [7]. Because most multilayer interfaces are made with hetero-junctions, detailed understanding of the various phenomena at the interface is crucial to improve the device performance [8]. For these reasons, many researchers have made efforts to control and understand these phenomena by theoretical and experimental approaches. As the scale goes down to atomic level, even the influence of the lattice mismatch and the stacking sequence at the interfaces were considered for the case of Fe and Al [9]. And using molecular dynamics simulation, Weng et al. investigated the influence of

incident energy on the deposited film surface property for both vertical and oblique deposition and found the incident energy for optimal film morphology for the case of Co on Cu substrate [10].

Previously we have investigated deposition behavior in the Co/Al system using molecular dynamics simulation. In the course of the investigation, although the incident energy of a Co atom was only 0.1 eV, we could observe surface alloying at the interface for various Al surface orientations [11]. It was reported that the formation of interface mixing could be successfully explained by the high value of the local acceleration due to the strong affinity between Co and Al and by the low activation barrier [12]. Consistent with this result, Mitsuzuka et al. reported that a nonmagnetic CoAl compound was formed at each interface of the Co/Al multilayer [13].

However, A/B/A structured multilayers have not been substantially investigated for the separate cases of A on B (A/B) and B on A (B/A). The results of Hafel et al. support this point of view and emphasize the necessity of investigations on different deposition cases in comparing Pt on Au(100) with Au on Pt(100) [14]. In general, growth mechanisms have been predicted by differences in surface free energy between

\*To whom all correspondence should be addressed. E-mail: yongchae@hanyang.ac.kr

deposited and substrate materials. The surface free energies of Pt and Au are 2.691 and 1.626 J/m<sup>2</sup> respectively [15]. Therefore, the difference of surface free energy in the case of A/B and B/A could explain the contrasting growth behavior. In the case of Co-Al especially, the surface free energy of Co is about three times higher than that of Al ( $\gamma_{\text{Co}} = 2.709$  J/m<sup>2</sup>,  $\gamma_{\text{Al}} = 1.085$  J/m<sup>2</sup>) [15], and it is generally known that the Co-Al system forms a stable intermetallic compound of B2 (CsCl) structure in the bulk phase. Moreover, the electro-magnetic properties of the CoAl compound are very peculiar compared with pure Co and Al [16]. In the present work we used molecular dynamics simulations to investigate the deposition and thin film growth behavior for both the Co/Al and Al/Co cases. Finally, guidelines to produce optimized interface structures of Al/Co/Al multilayer have been proposed.

## 2. Calculation Procedure

The embedded-atom method (EAM) based on interatomic potentials was utilized [17]. In the present work, we employed the potential developed by Pasianot and Savino for Co-Co [18], and Voter and Chen potential for Al-Al [19]. The pair potential of Co-Al was obtained by a linear combination of the effective pair interactions given by the following formula [20]:

$$V_{\text{CoAl}}^{\text{eff}}(a + bx) = A[xV_{\text{Al}}^{\text{eff}}(c + dx) + (1 - x)V_{\text{Co}}^{\text{eff}}(e + fx)] \quad (1)$$

where  $x$  takes values from zero to unity and the corresponding parameters are listed in Table 1. The Co-Co, Al-Al, Co-Al potentials employed showed good agreement with the experimental values of pure elements as well as those for intermetallic properties between atoms.

The substrate contained 1440 atoms with the planes normal to the surface forming ten layers of (001) planes containing 144 atoms each. The substrate dimensions were  $12a_0 \times 6a_0 \times 5a_0$ , where  $a_0$  was the bulk lattice constant for the surface normal to the  $z$  direction.

*Table 1.* Parameters for Co-Al interatomic pair potential. Energies are in eV, distances in Å.

a	b	c	d	e	f	A
1.690	4.0	1.910996	3.643984	1.75373	3.509799	1.0909091

Periodic boundary conditions were utilized in the  $x$  and  $y$  directions. To mimic a surface, the position of the bottom-most two layers was fixed and the substrate was kept at 300 K using the atom-velocity-rescaling method. The adatoms were randomly positioned in the  $xy$  plane at a distance of 30 Å from the substrate surface. The initial velocity of each incident atom can be calculated from the incident energy by the following expression:

$$V_{\text{adatom}} = \sqrt{\frac{2K_i}{M}} \quad (2)$$

where  $K_i$  represents the incident kinetic energy and  $M$  is the atomic mass. The MD time step was set to 1 femto-second (fs), and the system was fully relaxed for each additional adatom in the limit of 5 pico-second (ps). The XMD 2.5.32 code of Rifkin et al. was utilized for the MD simulation [21].

## 3. Results and Discussion

Figure 1 is the atomic configurations after Co atoms were deposited on Al(001) up to 10 mono layers (ML) with 0.1, 1.0, 3.0, and 5.0 eV of incident energy ( $K_i$ ), respectively. In the case of 0.1 eV, well-ordered mixing layers were formed at the Co/Al interface. This behavior is very similar to “bilayer growth” or “intermixed Stranski-Krastanov growth” reported by Fenter et al. [22] and Rousset et al. [23] in which gold atoms are intermixed with the silver atoms in the top two layers. Moreover, in our study a crystalline CoAl compound with the B2 (CsCl) structure seemed to be formed at the Co on Al(001) interface. This was probably due to the less than 0.1% lattice mismatch between the Al(001) surface and the CoAl (001) [11]. On increasing the  $K_i$ , however, well ordered structures gradually disappeared and the range of the amorphous mixing regions was extended.

Such a tendency could be clearly seen from the layer coverage of the Co/Al system shown in Fig. 2. Based on the results of Fig. 1. Figure 2 shows a comparison of layer coverage fraction of Co and Al atoms with distance along the [001] direction. The height was normalized to the initial surface of the Al(001) substrate, and 100% layer coverage corresponds to the 144 atoms occupying that layer irrespective of the atom types. As can be shown in Fig. 2(a), the incident Co atoms with 0.1 eV of incident energy resulted in alternating mixing

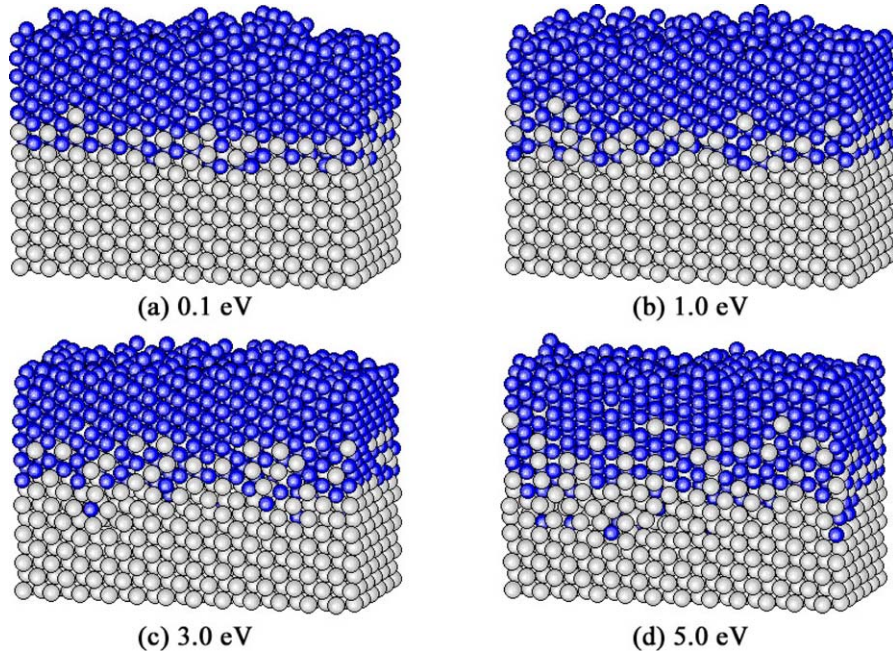


Fig. 1. The atomic configurations after deposition of Co on Al(001) up to 10 mono layers (ML) with respect to the incident energy; (a) 0.1 eV, (b) 1.0 eV, (c) 3.0 eV, and (d) 5.0 eV.

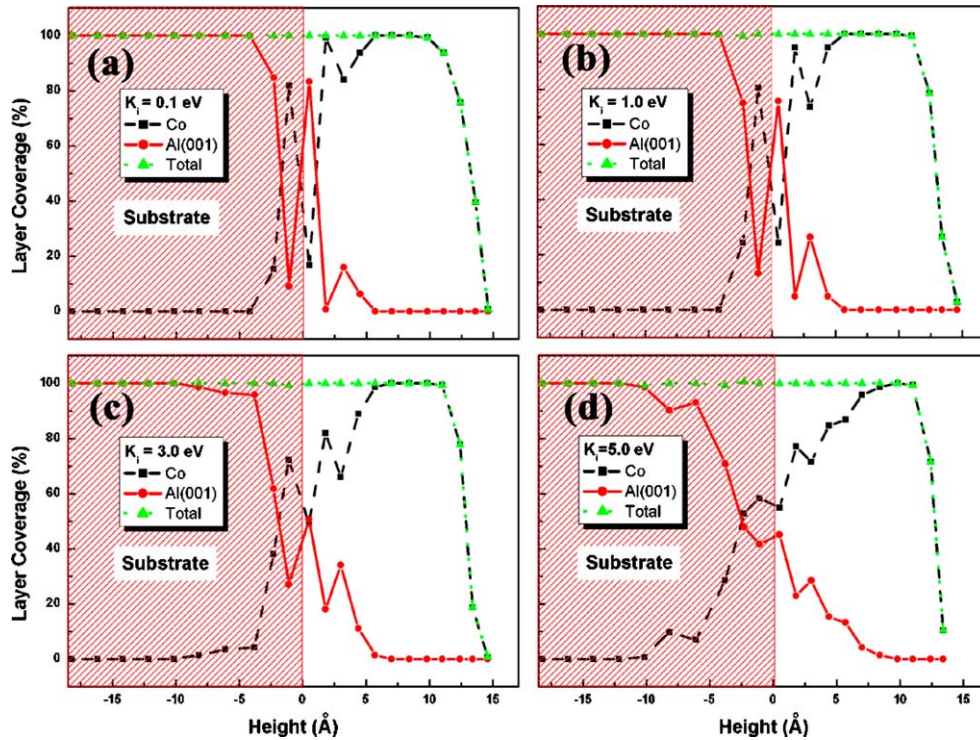


Fig. 2. Layer coverage fraction of Co on Al(001) surface along the [001] direction, 10 ML of Co atoms were deposited on Al surface with respect to the incident energy; (a) 0.1 eV, (b) 1.0 eV, (c) 3.0 eV, and (d) 5.0 eV.

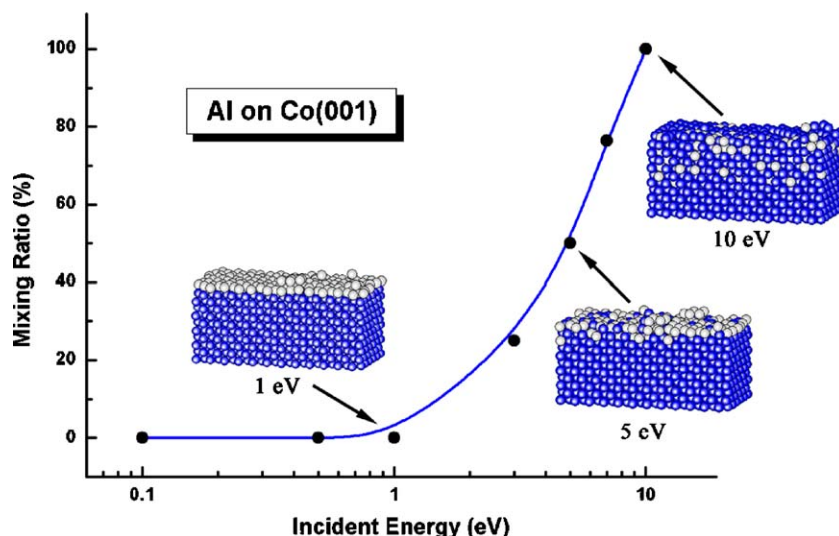


Fig. 3. Degree of mixing ratio of Al on Co(001) with respect to various incident energies ( $K_i$ ) after deposition of 1 ML of Al (corresponding to 144 atoms).

layers of Co and Al on Al surface, and this mixing layer was turned out to be a B2 structure. As the  $K_i$  increased, the alternation of layer coverage of Co and Al atoms was decreased, and the thickness of mixing regions was simultaneously extended. In the case of 5.0 eV [Fig. 2(d)], the mixing layers reached to 2 nm at the Co/Al interface. Interestingly, the roughness of the deposited Co thin film was decreased with respect to the increasing  $K_i$ .

Figure 3 shows the mixing ratio for the case of Al on Co(001) as the  $K_i$  increments from 0.1 to 10.0 eV. As indicated elsewhere, for Co on Al(001), 90% of the Co atoms were found to be mixed with the Al(001) substrate even when the lowest incident energy of 0.1 eV [11]. In the case of Al on Co(001), however, no mixing layers were formed at the interface, and a sharp interface could be seen instead at 0.1 eV of incident energy. Although the region with 50% mixing ratio was observed for 5.0 eV Al atoms, the structure of the mixing layers was entirely different from the former case of Co/Al(001). A  $K_i$  of at least 7.0 eV was found to be necessary to form the layer of 90% mixing ratio. In the case of 10.0 eV, almost all the Al atoms were mixed with the Co(001) substrate, and they were located at the substitutional site of the Co(001). These results are in sharp contrast to the results of Co on Al(001). Although the CoAl is a stable phase, no CoAl compound layers were formed at the interface.

This different behavior could be explained by the much higher activation energy barrier for the incorporation of adatoms into the substrate in the Al/Co(001) case than that for the Co/Al(001) case.

Table 2 shows the interfacial roughness ( $R$ ) for Co/Al(001) and Al/Co(001) with different incident energies. The interfacial roughness can be used to quantify the degree of interface roughness, and is calculated as follows [24]:

$$R = \sqrt{\frac{\sum_{j=0}^n (Z_j - \bar{Z})^2}{n}} \quad (3)$$

where  $n$  is the total number of atoms which lie in the interfacial positions,  $j = 0$  corresponds to the interfacial layer,  $\bar{Z}$  represents the mean height of the film surface, and  $Z_j$  represents the height of the mixed atoms. Perfectly separated interface corresponds to '0' and the degree of the roughened or mixed interface

Table 2. Estimated interfacial roughness for Co/Al(001) and Al/Co(001) with different incident energies.

$K_i$	0.1 eV	1.0 eV	3.0 eV	5.0 eV
Co/Al	2.002	2.164	2.898	4.023
Al/Co	0.094	0.091	1.303	1.886

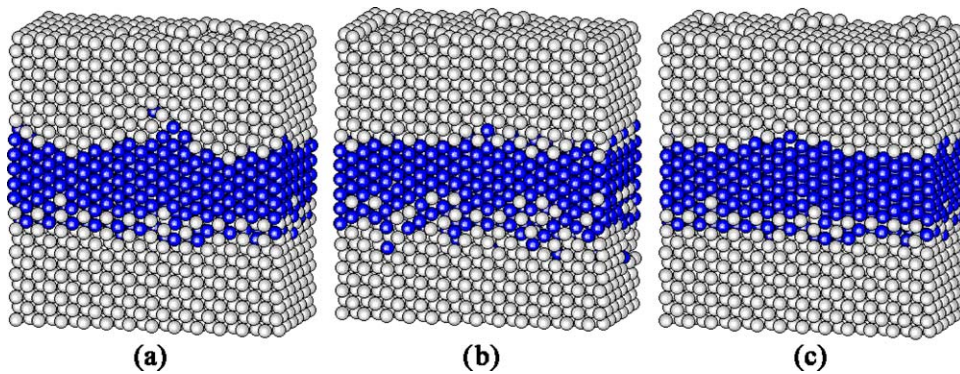


Fig. 4. Al(10 ML)/Co(10 ML)/Al(001) multilayers fabricated by various procedures; (a) Incident energy at 0.1 eV throughout the deposition, (b) Incident energy at 3.0 eV throughout the deposition, and (c) First 5 ML of Co with 0.1 eV and additional 5 ML with 3.0 eV.

is in proportion to this value. The interfacial roughness values, listed in Table 2, represent the different behavior for Co/Al(001) and Al/Co(001). In the case of Co/Al(001), the value was nearly 2.00 at 0.1 eV incident kinetic energy, which indicates mixed but highly ordered structure, B2 structure. As the  $K_i$  increased, these values increased continuously and interface structure became more roughened as shown in Fig. 1. In the case of Al/Co(001), however, the values were nearly 0.00 up to 1.0 eV incident kinetic energy, which means that interfacial mixing was hardly occurred as shown in Fig. 3.

Based on the above observations, atomic configurations for Al(10ML)/Co(10ML)/Al(001) sandwich structures for various  $K_i$  values were tested (Fig. 4). These are very similar to the proposals of Zhou et al. [25]. Figure 4(a) is the case that the  $K_i$  was fixed at 0.1 eV over the entire deposition process, and Fig. 4(b) is the case for 3.0 eV. In the case of 0.1 eV, well-ordered B2 structures were formed at the Co/Al(001) interface, but the Al/Co(001) interfaces that formed were highly roughened. Nevertheless, mixing layers were hardly formed at the Al/Co interface, and Al adatoms were grown epitaxially on the roughened Co surface. In the case of 3.0 eV, however, more disordered mixed layers, not highly ordered B2 structure, were formed at the Co/Al(001) interface. However, due to the relatively high  $K_i$ , the surface of the Co thin film seemed to be flattened, and a highly straight Al/Co interface could be obtained. Figure 4(c) is the configuration in which the weak points of former two cases have been addressed. At first, 5 ML of Co were formed with a low  $K_i$  of 0.1 eV to avoid the disordered structures at the inter-

face and an additional 5 ML were then deposited with a relatively high  $K_i$  of 3.0 eV to avoid roughening of the surface.

#### 4. Conclusions

Using molecular dynamics simulations, we undertook a systematic investigation of the thin film growth behavior for Co/Al(001) and Al/Co(001). In the case of Co on Al(001), CoAl (B2 structure) intermixed layers were formed for a low incident energy of 0.1 eV. Increasing the incident energy produced more disordered and thicker mixing layers. In the case of Al on Co(001), however, no intermixed layers were formed until 1.0 eV, and, at  $K_i$  over 5.0 eV, intermixed layers of 50% mixing ratio could be found. Consequently, procedures for optimized multilayer structures of Al/Co/Al by controlling the incident energy of adatoms were proposed.

#### Acknowledgment

The authors would like to acknowledge the support from the KISTI (Korea Institute of Science and Technology Information) under ‘The Fifth Strategic Supercomputing Support Program’ with Dr. Sang Min Lee as the technical supporter. The use of the computing system of the Supercomputing Center is also greatly appreciated. (S.-P.K. and Y.-C.C.) This work was also supported by KIST Vision 21 on ‘A study on the basic technology of nano-spin function device’ with contact no. 2E17712 (S.-P.K., S.C.L. and K.R.L.)

## References

1. J. Enkovaara, A. Ayuela, and R.M. Nieminen, *Phys. Rev. B*, **62**, 16018 (2000).
2. J.M. Pruneda, R. Robles, S. Bouarab, J. Ferrer, and A. Vega, *Phys. Rev. B*, **65**, 0244401 (2001).
3. H. Arduin, E. Snoeck, and M.-J. Casanove, *J. Crystal Growth*, **182**, 394 (1997).
4. A. Wiessner, M. Agne, D. Reuter, and J. Kirschner, *Surf. Sci.*, **377–379**, 937 (1997).
5. S. Oikawa, A. Shibata, S. Iwata, and S. Tsunashima, *J. Magn. Magn. Mater.*, **177–181**, 1273 (1998).
6. M. Benaissa, P. Humbert, H. Lefakis, J. Werckmann, V.S. Speriosu, and B.A. Gurney, *J. Magn. Magn. Mater.*, **148**, 15 (1995).
7. K. Inomata and Y. Saito, *J. Appl. Phys.*, **81**, 5344 (1997).
8. J.M. de Teresa, A. Barthélémy, A. Fert, J.P. Contour, F. Montaigne, and P. Seneor, *Science*, **286**, 507 (1999).
9. A. Fuß, S. Demokritov, P. Grünberg, and W. Zinn, *J. Magn. Magn. Mater.*, **103**, L221 (1992).
10. C.-I. Weng, C.-C. Hwang, C.-L. Chang, J.-G. Chang, and S.-P. Ju, *Phys. Rev. B*, **65**, 195420 (2002).
11. S.-P. Kim, S.-C. Lee, K.-R. Lee, Y.-C. Chung, and K.-H. Lee, *J. Appl. Phys.*, **93**, 8564 (2003).
12. S.-P. Kim, S.-C. Lee, K.-R. Lee, and Y.-C. Chung, *J. Korean Phys. Soc.*, **44**, 18 (2004).
13. T. Mitsuzuka, A. Kamijo, and H. Igarashi, *J. Appl. Phys.*, **68**, 1787 (1990).
14. M.I. Haftel, M. Rosen, T. Franklin, and M. Hettermann, *Phys. Rev. B*, **53**, 8007 (1996).
15. L.Z. Mezey, and J. Giber, *Jpn. J. Appl. Phys.*, **21**, 1569 (1982).
16. J.Y. Rhee, Y.V. Kudryavtsev, K.W. Kim, and Y.P. Lee, *J. Appl. Phys.*, **87**, 5887 (2000).
17. M.S. Daw and M.I. Baskes, *Phys. Rev. Lett.*, **50**, 1285 (1983).
18. R. Pasianot and E.J. Savino, *Phys. Rev. B*, **45**, 12704 (1992).
19. A. Voter and S. Chen, *Mater. Res. Soc. Symp. Proc.*, **82**, 175 (1987).
20. C. Vailhé and D. Farkas, *J. Mater. Res.*, **12**, 2559 (1997).
21. J. Rifkin, *XMD Molecular Dynamics Program* (Univ. of Connecticut, 2002).
22. P. Fenter and T. Gustafsson, *Phys. Rev. Lett.*, **64**, 1142 (1990).
23. S. Rousset, S. Chiang, D.E. Fowler, and D.D. Chambliss, *Phys. Rev. Lett.*, **69**, 3200 (1992).
24. M.-H. Su, C.-C. Hwang, J.-G. Chang, and S.-H. Wang, *J. Appl. Phys.*, **93**, 4566 (2003).
25. X.W. Zhou, H.N.G. Wadley, R.A. Johnson, D.J. Larson, N. Tabat, A. Cerezo, A.K. Petford-Long, G.D.W. Smith, P.H. Clifton, R.L. Martens, and T.F. Kelly, *Acta Mater.*, **49**, 4005 (2001).